ELSEVIER

Journal of Atmospheric and Solar-Terrestrial Physics 67 (2005) 839–852

Journal of ATMOSPHERIC AND SOLAR-TERRESTRIAL PHYSICS

www.elsevier.com/locate/jastp

A statistical study of magnetic cloud parameters and geoeffectiveness

E. Echer*, M.V. Alves, W.D. Gonzalez

Instituto Nacional de Pesquisas Espaciais (INPE), Av. Astronautas, 1758, ZIP: 12201-970, São José dos Campos, SP, Brazil

Received 10 February 2004; received in revised form 31 August 2004; accepted 25 February 2005
Available online 23 May 2005

Abstract

A statistical study of magnetic cloud parameters and geoeffectiveness is presented in this work, based on the analysis of 149 magnetic clouds during the period 1966–2001. The distributions of maximum magnetic field strength, solar wind speed and southward magnetic field inside the clouds were determined for the whole data set and for subsets classified according to the magnetic cloud polarity (rotation in Z or Y directions). The geoeffectiveness was determined by classifying the number of magnetic clouds followed by intense, moderate and weak magnetic storms, and by calm periods. It was found that around 77% of the magnetic clouds are geoeffective, i.e., they were followed by intense or moderate geomagnetic storms ($Dst \leqslant -50\,nT$). Considering also weak storms ($Dst \leqslant -30\,nT$), 97% of MCs were followed by geomagnetic activity. When considering polarity, each magnetic cloud subset has a slightly different geoeffectiveness, which is in agreement with the differences observed in their parameter distributions. The NSY_- was observed to be the less geoeffective of the MC subsets, with 66.6% of this class events being followed by intense or moderate storms, against 73.0% of SNY_+, 80.0% of the Y, 83.3% of the NSY_- and 85.7% of the SNY_-. The B_{peak}–V_{peak} relation was confirmed for the magnetic clouds with rotation in Z direction.

Keywords: Magnetic clouds; Solar wind; Geomagnetic storms; Space weather

1. Introduction

The existence of certain volumes of plasma moving at high speeds from the Sun to Earth to explain intense geomagnetic storms has been postulated long before the space age. According to Burlaga (1995) this concept was introduced in the early 1930s (Chapman and Ferraro, 1931; Gold, 1959, 1962). The observation of the interplanetary remnants of solar ejecta and their main characteristics was inferred in the early epoch of solar wind observations (Gosling et al., 1973). These flows were called clouds, plasma clouds, nascent streams, flare streams, magnetic tongues, jets, magnetized plasma clouds, bottles, and bubbles. After observations in situ, such flows have been called postshock flows, drivers, transients, plasma clouds, flare ejecta, coronal mass ejections (CMEs), interplanetary CMEs (ICMEs), ejecta, and magnetic clouds (MCs). According with the American Geophysical Union (AGU) index set, the term ejecta is used for interplanetary flows and CMEs for the mass ejection that can be seen moving away from the Sun with a coronagraph (Burlaga et al., 2001). In this paper, we will use the term ICMEs to designate the interplanetary manifestations of CMEs. By the early 1980s, most of the characteristic signatures of ICMEs, plasma and field properties, have been identified (see e.g.

*Corresponding author. Tel.: +55 12 3945 6797; fax: +55 12 3945 6810.
E-mail address: eecher@dge.inpe.br (E. Echer).

1364-6826/$ - see front matter © 2005 Elsevier Ltd. All rights reserved.
doi:10.1016/j.jastp.2005.02.010

Gosling, 1997; Neugebauer and Goldstein, 1997). Among all signatures, the counterstreaming suprathermal electrons seem to provide the most unambiguous indication of ICMEs (Gosling et al., 1987).

Some of the historical terms mentioned previously are related with the plasma and field properties of the observed structure. It has been postulated that if the ICMEs are attached to the Sun one can have the magnetic "tongue" structure (Gold, 1962). If the fields are closed, one has a cloud or magnetic bubble structure (Gonzalez et al., 1994). Gosling et al. (1973) have observed the occurrence of low proton temperature T_p in solar wind after shocks and postulated the existence of magnetic bottles. Bame et al. (1979) presented a visualization of the evolution of the ICMEs in interplanetary space and described the driver gas region as being characterized by low solar wind proton density and temperature and intense and smooth magnetic fields (see also Tsurutani et al., 1990). Frequently there is also a lumpy distribution of enriched helium present (Zwickl et al., 1983; Hirshberg et al., 1972). Sometimes, within the driver gas, strong north–south interplanetary magnetic field (IMF) components occur. This occurs mainly in the low plasma beta region, where magnetic fields are relatively free of discontinuities and angular changes/waves occur slowly (Zwickl et al., 1983; Tsurutani et al., 1988). Choe et al. (1982) have found within the driver gas an interval of low beta of 0.03–0.8, with 0.1 typical. This region of space is frequently characterized by a bi-directional electron/proton streaming (Gosling et al., 1987). These regions of large variations in NS direction are called magnetic clouds after Burlaga et al. (1981). Goldstein (1983) and Marubashi (1986) presented the field configuration of MCs as a giant flux rope, with force free fields generated by field aligned currents along the MC axis.

We will consider MCs as a subset of ICMEs (Klein and Burlaga, 1982). These structures, MCs, are identified near 1 Astronomical Unit (AU) by (1) large-scale smooth field rotations, (2) enhanced magnetic field magnitude, and (3) decreased plasma temperatures (e.g., the review by Burlaga (1991) and references therein). MCs present dimensions around 0.2–0.3 AU, and cross the spacecraft/Earth in 24 h (Burlaga et al., 1981; Lepping and Berdichevsky, 2000). While only 10% of all ICMEs identified with counterstreaming halo electrons fit the above definition of MCs, with magnetic field strength higher than 10 nT, roughly 1/3 of all ICMES exhibit at least the large smooth field rotation characteristics of MCs (Gosling et al., 1990).

Since MCs are an important source of southward interplanetary magnetic field, the relation between MCs and geomagnetic storms have been investigated by several authors (Burlaga et al., 1981; Klein and Burlaga, 1982; Gonzalez and Tsurutani, 1987; Tsurutani et al., 1988, 1992; Farrugia et al., 1995; Lepping and Berdichevsky, 2000; Dal Lago et al., 2000, 2001; Wu and Lepping, 2002a, b; Lepping et al., 2003).

In this work, a statistical study of the MC parameters and their geoeffectiveness is performed for the whole solar wind observation period. A large number of magnetic clouds, 149, were analyzed during the 1966–2001 period, and the whole data set as well the subsets defined by the polarization of magnetic cloud, are studied.

2. Methodology of analyses

Magnetic clouds were selected through lists of ICMEs events available in the literature (Klein and Burlaga, 1982; Marsden et al., 1987; Bothmer and Rust, 1997; Bothmer and Schwenn, 1998; Bravo and Blanco-Cano, 1998; Crooker et al., 1998; Bravo et al., 1999; Blanco-Cano and Bravo, 2001; Magnetic clouds table on-line http://lepmfi.gsfc.nasa.gov/mfi/mag_cloud_pub1.html, 2002). From these references, all ICMEs events were analyzed by looking in plots generated from OMNIweb database. Some events presented large data gaps, due to the sparse coverage of solar wind. These events were not considered for further analyses. Other events were analyzed and MCs were identified using the criteria: (i) high magnetic field strength; (ii) smooth rotation in the B_z or B_y component; (iii) low proton temperature and beta (Burlaga et al., 1981; Burlaga, 1995). Using these criteria a total of 149 MCs events were selected in order to perform the study. Since our main interest is to verify the geoeffectiveness of MCs, we have not considered the ones that present B_y rotation with B_z to north, which are, in general, not geoeffective (in terms of the ejecta field). The Geocentric Solar Magnetospheric coordinates were used in this study.

Some difficulties were found conducting this analysis, which was expected. MCs are very large structures and only one point of observation is available, the spacecraft, which sometimes cross the ejecta far from the main axis (Gonzalez et al., 1999). Another point is that the magnetic cloud axis is not perfectly aligned (rotation in Z) or perpendicular (rotation in Y) to the ecliptic plane, with several possible intermediate inclinations (Gonzalez et al., 1990). It was observed in some events a rotation both in Y and in Z directions. In these cases, the polarity of the cloud was defined according to the component with the highest variation.

According to polarity, magnetic clouds were classified in: NS-Y_+ (B_z component rotating from north to south, with B_y component in the East/+ direction); NS-Y_- (B_z component rotating from north to south, with B_y component in the West/− direction); SN-Y_+ (B_z component rotating from south to north, with B_y component in the East/+ direction); SN-Y_- (B_z component rotating from south to north, with B_y component in the West/− direction); Y-S

(B_y component rotating east to west or west to east direction, with B_z component in the south direction).

The ring current Dst index was introduced in 1964 and it primarily measures the effects of ring current in the geomagnetic field. It is based on hourly averages of the horizontal component recorded at four low-latitude observatories, subtracting the average solar quiet variation and the permanent magnetic field from the disturbed one. It is available since 1957 (Sugiura, 1964). The hourly Dst index, for the studied period, was obtained from the World Data Center for Geomagnetism, Kyoto. In order to classify the MC geoeffectiveness, the Dst peak during the MC passage through Earth was taken, and the geomagnetic activity level was classified in intense, $\mathrm{Dst} \leqslant -100$, moderate, $-100 < \mathrm{Dst} \leqslant -50$, or weak activity, $-50 < \mathrm{Dst} \leqslant -30$, and in quiet periods, $\mathrm{Dst} > -30$ (Gonzalez et al., 1994).

As an example of the data that have been used in this work, Fig. 1 shows a magnetic storm caused by a magnetic cloud in the period April 16–17, 1999. Panels are, from top to bottom: solar wind proton temperature T_p, solar wind speed V_{sw}, solar wind proton density N_p, interplanetary magnetic field magnitude B and components (in geocentric solar magnetosphere coordinates—GSM) B_x, B_y and B_z, plasma proton β, and the geomagnetic symmetric index Sym-H. This index is derived similarly to the Dst, but with a 1-min high-resolution sampling. The solid line indicates the shock and the magnetic cloud boundaries are delimited by the dotted lines. Between the shock and the magnetic clouds is the sheath region, where the plasma has turbulent variations, because it was compressed and heated by the shock. The increased dynamic pressure caused a very impressive enhancement in the magnetopause Chapman–Ferraro current, as seen by the increase in the Sym-H index. This particular MC is of the type SN, i.e., the B_z component shows a rotation from south to north, with the B_y component remaining most of the time positive. Although in this paper we do not make a difference if the geomagnetic storm is caused by the MC itself or by the sheath region, in this example it was the S field in the cloud that produced the geomagnetic storm, with Dst peak of -91 nT. The Sym-H peak is higher (-123 nT) because Dst is a 1 h average value, smoothing large extreme in 1 min data. In a recent paper, Li and Luhmann (2004), examined how significantly the MC portion of the disturbed period contributes to the geoeffectiveness.

3. Results and discussion

3.1. Results for the whole set

The peak values within each MC, not including the sheath region, of magnetic field strength, B_{peak}, of solar wind speed V_{peak}, southward magnetic field component, Bs_{peak} and of Dst_{peak} have been determined. Table 1 shows the statistics of these parameters for the 149 MCs data set, presenting the average value as well the standard deviation, and the maximum and minimum value for each parameter. It is also included in Table 1 the percentage of the Bs_{peak} in relation to the total B_{peak}. The distributions for these parameters are shown in Fig. 2.

The average value for B_{peak} is 15.5 nT, with extrema 5.2 and 37.0 nT. The distribution seen in Fig. 2 is asymmetric, showing a peak between 10 and 15 nT and decreasing for extreme values. The Bs_{peak} distribution shows a similar behavior, with distribution maximum between -5 and -10 nT and average around -10 nT. The percentage of Bs_{peak} in relation to B_{peak} is close to 70%. The distribution of solar wind maximum speed inside the MCs shows three peaks between 400 and 550 km/s, with the peak closer to 400 km/s presenting the highest occurrence. The average for V_{peak} is 485 km/s. The average storm intensity as quantified by Dst_{peak} is -94 nT, indicating moderate geomagnetic activity. Dst_{peak} distribution has two peaks, around -30 and -90 nT.

An analysis of the time profiles for the B_s/B ratio for 13 MCs was conducted by Dal Lago et al. (2000). They have concluded that during a large fraction of the MC time crossing through the spacecraft, more than 60% of the B value is in the Z direction. Tsurutani et al. (1988, 1992) have also observed that magnetic clouds, during more than half time of its duration, show B_z southward of the order of 70% of the B, or even more. In this work only the peak percentage is being considered, not the average or the entire profile inside the MCs, but it can be concluded that percentages around 70% of the total magnetic field in the southward direction are a confirmed characteristic of magnetic clouds.

It has been noticed that, in general, slow ICMEs, which usually do not form shocks, are not followed by intense geomagnetic storms. However, recently, Tsurutani et al. (2004) have shown that sometimes slow ICMEs do form shocks. They have defined "slow" ICMEs as the ones with core speed <400 km/s. They have found that 5 of 27 events were led by shocks, from which 4 were weak shocks. Also 5 MCs were followed by intense magnetic storms due to intense and/or long duration electric fields within the MCs. They have observed also that these slow MCs do not follow the linear $B_{peak} \times V_{peak}$ relationship. Their B_{peak} distribution has maximum around 13 nT and Bs_{peak} has maximum around 7–11 nT. Nevertheless, most of slow MCs were neither led by shocks nor caused intense geomagnetic storms.

Initially, there was no physical justification of why these low-speed ejecta could not have intense magnetic fields. Gonzalez et al. (1998) analyzed two different

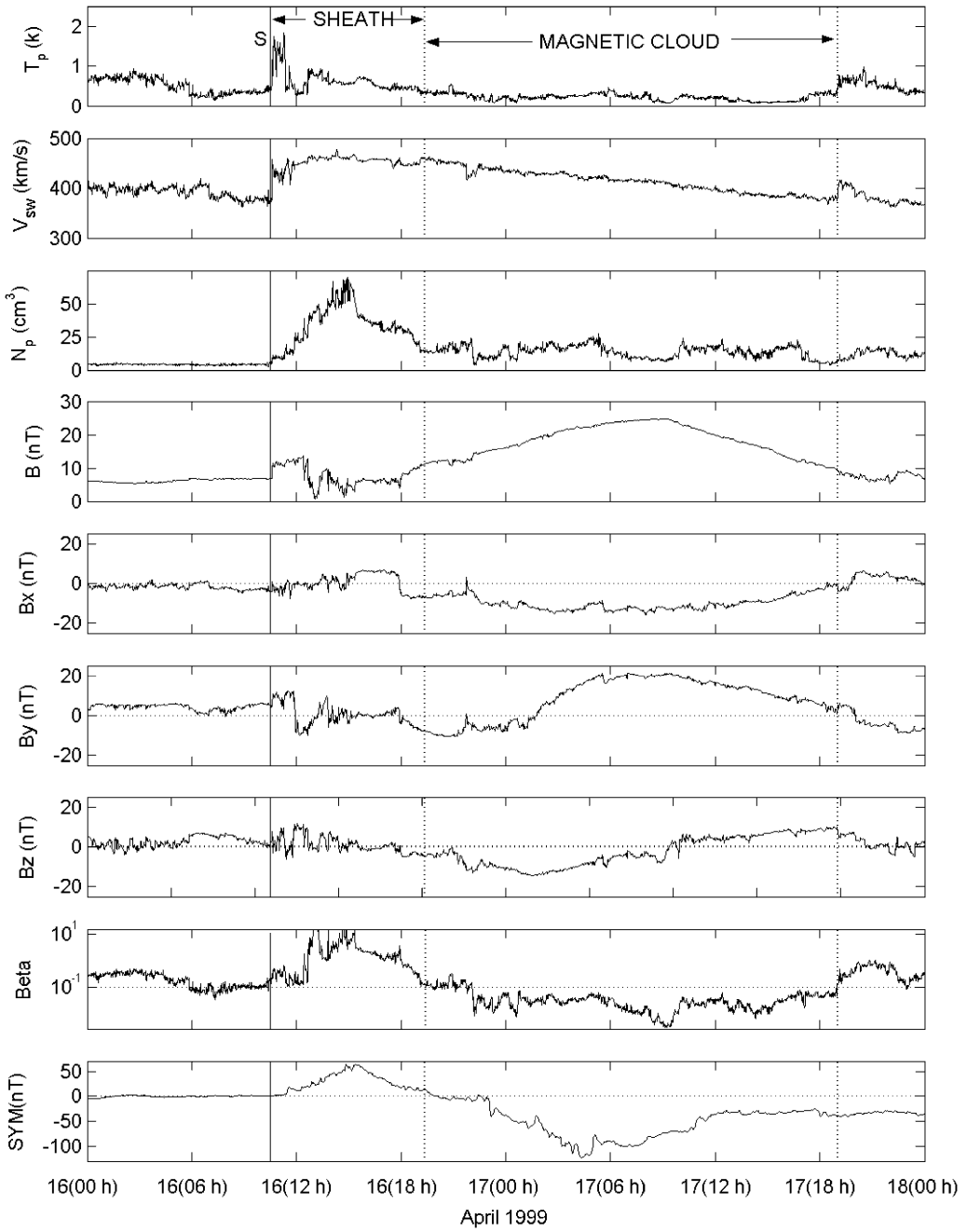

Fig. 1. Example of a magnetic cloud SN Y_+ observed by ACE spacecraft in April 16–17, 1999. Panels are, from top to bottom: solar wind proton temperature T_p, solar wind speed V_p, solar wind proton density N_p, interplanetary magnetic field magnitude B and components (in GSM) B_x, B_y and B_z, plasma proton Beta and the geomagnetic symmetric index Sym. The shock is indicated by the solid line, and the sheath and magnetic cloud regions are labeled.

magnetic cloud sets and 1 set of ICMEs no-MCs. They concluded that it is possible to obtain a $B_{peak} \times V_{peak}$ relation, written as $B_{peak} = a + bV_{peak}$ only for the MC sets. They obtained for their data set the following equation: $B_{peak} = -1.1 + 0.047V_{peak}$ with a correlation of $r = 0.71$. This relation is a clear trend that MCs with higher velocities will have higher B. Gonzalez et al. (1998) have commented that, since fast MCs are

followed by moderated and intense geomagnetic storms, this would occur because of their high magnetic fields. The absence of intense storms following slow ejecta could then be accounted by their low magnetic field magnitudes. Further works have confirmed this general relation (Marubashi, 1998; Dal Lago et al., 2001). Owens and Cargill (2002) have found the same coefficient $b = 0.047$ in their analysis of the solar wind disturbed with $B > 18$ nT during more than 3 h. However, their analysis was not restricted to MCs.

Fig. 3 shows the $B_{peak} \times V_{peak}$ relation for the 149 MCs selected for this work. The equation we found for the data is $B_{peak} = 5.5 + 0.020 V_{peak}$, with $r = 0.35$, different from the one found by Gonzalez et al. (1998). Dal Lago et al. (2001) have analyzed 54 magnetic clouds, not including in their data the ones compressed by corrotating high-speed streams. They have found an equation given by $B_{peak} = 6.2 + 0.024 V_{peak}$, with $r = 0.60$. This equation is very similar to the one presented here, including the angular coefficient, b, 0.024 against 0.020. These coefficients indicate that, for each 100 km/s of increase in V_{peak}, an increase between 2.0 and 2.5 nT in the B_{peak} would be expected, against an increase of 4.7 nT predicted by the Gonzalez et al. (1998) relation.

Table 1
Statistics of the whole magnetic cloud data set

Parameter	Average/SD	Minimum	Maximum
B_{peak}	15.5 ± 5.9 nT	5.2 nT	37.0 nT
V_{peak}	485 ± 101 km/s	325 km/s	820 km/s
Bs_{peak}	-10.5 ± 5.2 nT	-31.0 nT	-2.4 nT
Dst_{peak}	-93.8 ± 55.0 nT	-288 nT	-5 nT
Perc. (Bs_{peak}/B_{peak})	$67.8 \pm 19.3\%$	15.2%	100%

The discrepancy in the coefficients seems to be due to the number of events and the criteria used to select them. While Gonzalez et al. (1998) have choose only 13 well-behaved MCs, both in Dal Lago et al. (2001) and in the present work a larger number of magnetic clouds were selected, including the ones when the satellite has crossed far from the axial direction. Particularly in this work, slow magnetic clouds, magnetic clouds compressed by corotating interaction regions (CIRs) high-speed streams and with rotation in Y have been used. In this sense, the present analyses is more complete, including a larger number of MCs. From this large

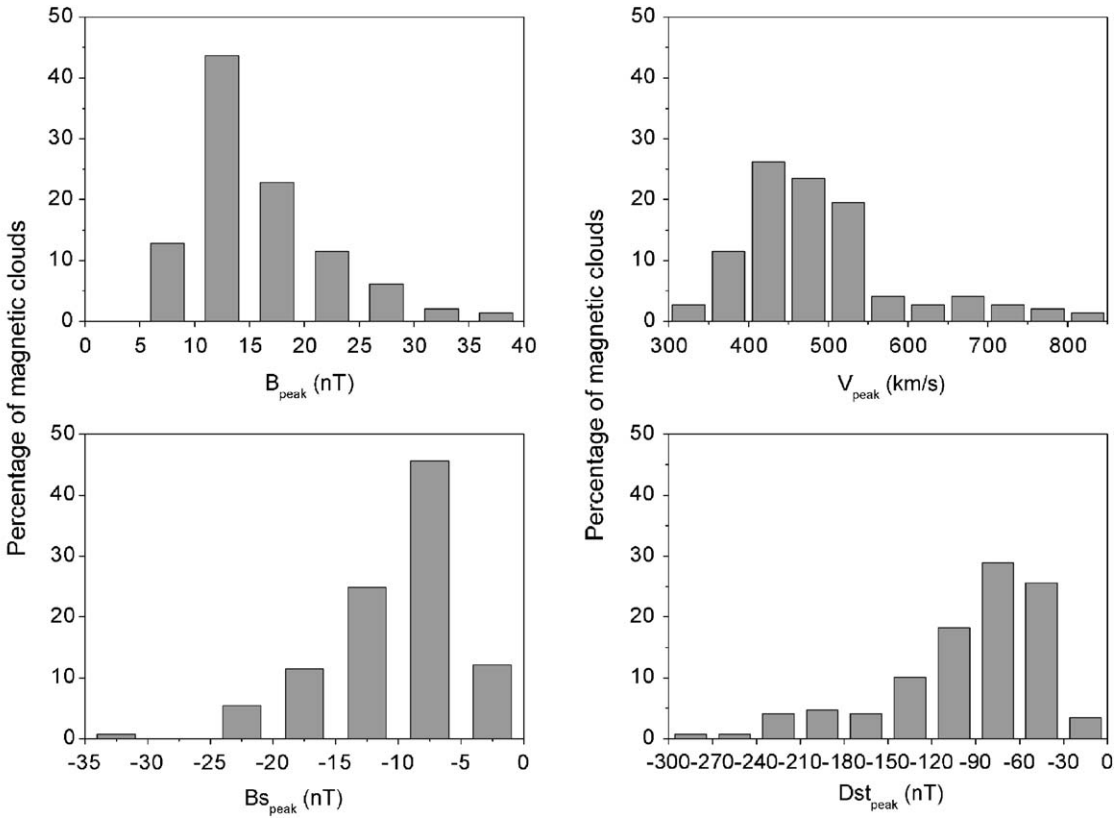

Fig. 2. Distribution of the peak values for B_{peak} (top panel on the left), V_{peak} (top panel on the right), Bs_{peak} (bottom panel on the left) and Dst_{peak} (bottom panel on the right) for the 149 magnetic clouds set.

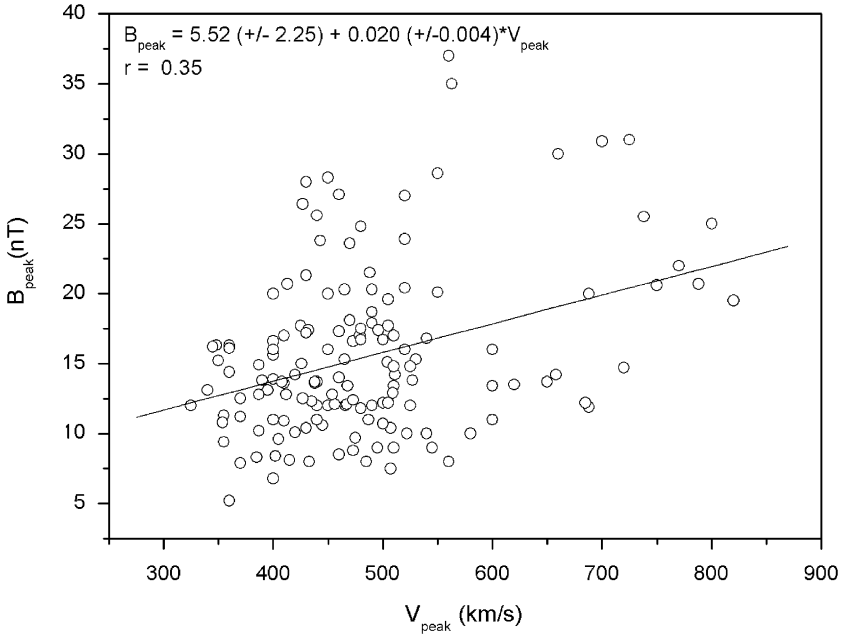

Fig. 3. Relation between B_{peak} and V_{peak} for the 149 magnetic clouds set.

MC data set analysis one can conclude: (i) although the correlation is low, the B_{peak}–V_{peak} relation is confirmed, i.e., its validity was extended; (ii) the angular coefficient is similar to the one found by Dal Lago et al. (2001) in an independent study, and seems to be more appropriated when one includes a large number of events crossed by the spacecrafts in different positions; (iii) the linear coefficient, a, could also have some physical significance: the coefficient around 5–6 nT observed in this work and in the one of Dal Lago et al. (2001) is very close to the background interplanetary magnetic field, around 5 nT (Parks, 1991). Considering that, the linear equation between B_{peak} and V_{peak} tells that, when the V_{peak} is zero, i.e., there is no mass ejection in the solar wind, the magnetic field is the one of the quiet solar wind.

From the 149 MCs data set, 18 were followed by CIR high-speed streams. When these 18 particular clouds are not included, the equation is $B_{peak} = 3.45 + 0.024 V_{peak}$ with $r = 0.42$. It is interesting to note that now the coefficient is exactly the same as the one found by Dal Lago et al. (2001), who have also not included the compressed MCs in their analysis.

The implication of this B_{peak}–V_{peak} proportionality for geoeffectiveness is that, for faster magnetic clouds, the magnetic field will be more intense, with a significative southward component, as pointed out above. Then the energy transfer from solar wind to the magnetosphere, controlled by the convection electric field $E_y = -VB_s$ (Gonzalez et al., 1994) is enhanced by both factor, V and B. This result excludes the possibility of a fast MC with low B causing intense geomagnetic storms (Gonzalez et al., 1998).

A possible physical mechanism responsible by this relation is presently not known. Compression of the cloud is occuring, but it is not possible to affirm that the increase in B should be attributed only to this effect. The mechanism of acceleration and liberation of ICMEs in the Sun could be partly responsible also for the higher magnetic field values (Gonzalez et al., 2001). Results from a numerical simulation by Wu and Guo (1997) showed that the radial velocity in the middle of the flux rope (magnetic cloud) erupting across a helmet streamer is proportional to the azimuthal B component.

The geoeffectiveness of the total MC set was evaluated, by determining the percentage of magnetic clouds that were followed by each type of geomagnetic activity. The storms were determined by looking in the Dst peak during or after the MC, thus the effect is not purely due to the MC fields; pre-existent B_s fields can be contributing. Many storms are known to have a double or triple phase, being caused by an association of fields (Kamide et al., 1998). Echer and Gonzalez (2004) have found that, for MCs associated with shocks, the percentage of geoeffective events is slightly higher (81%) then when considering all MCs, which indicates that the combined effect of sheath and MC fields leads to a higher number of MCs being followed by moderate + intense storms. Recently, Li and Luhmann (2004) have shown that half of the time the cloud portion of the disturbance provides the sole or major contribution to the resulting geomagnetic storm, and

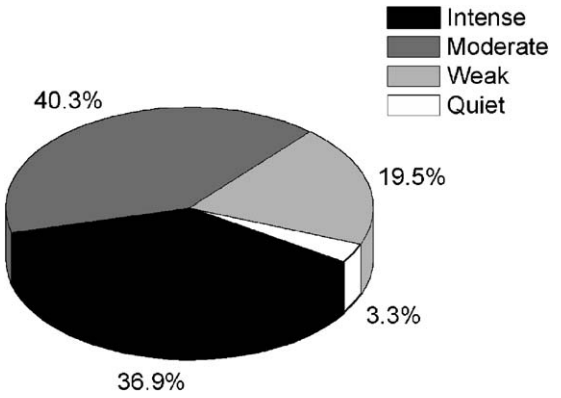

Fig. 4. Graph sector showing the percentage of magnetic clouds followed by each type of geomagnetic activity conditions for the 149 magnetic clouds set.

often (about 30% of the cases) the sheath portion of the MC period provides significant contribution to the storm. Wu and Lepping (2002a, b), analyzing 4 years of Wind data have shown that around 21% of the storms are caused by sheath plus MC fields.

Fig. 4 shows a sector graph of the distribution of magnetic clouds according to the geomagnetic level that followed each one. It can be seen that most of magnetic clouds cause intense or moderate magnetic storms (77.2% of the total). The small percentage of weak geomagnetic activity or quiet periods after MCs could be accounted by the presence of slow magnetic clouds, which have a lower total magnetic field and consequently a lower southward magnetic field, besides its lower speed. Consequently the convection electric field E_y would be lower. This statistic results confirms the strong geoeffectiveness of magnetic clouds.

3.2. Results for MC polarity subsets

Magnetic clouds with rotation in B_z and axial field in B_y are also called bipolar structures, being classified in SEN (SN-Y_+), SWN (SN-Y_-), NES (NS-Y_+), NWS (NS-Y_-). The MCs with rotation in B_y and axial field in B_z (Y-S, Y-N) are called unipolar structures (Gonzalez and Gonzalez, 1990; Mulligan et al., 1998).

From the whole data set of 149 MCs, 51 are of the type NS, 15 are Y-S, and 83 are of the type SN. Considering polarity, it was observed 27 MCs of type NS-Y_+, 24 MCs of type NS-Y_-, 48 MCs of the type SN-Y_+, 35 of the type SN-Y_-. Considering only the NS and SN clouds, one has a total of 134, from which 38% are of the type NS and 62% of the type SN.

In the analysis of MC polarity per solar cycle, it is important to remember that the period with larger number of solar wind observations was between 1978–1992 and 1995–2001, both periods of solar maximum. In the remaining of the period, observations are sparse, which makes a direct comparison, between maxima and minima solar cycles, difficult. The MC polarity percentage per solar cycle phase was determined and it is shown in Table 2. Results show that during periods close to odd solar cycle maxima—cycles 21 and 23, the SN MCs predominate, while during periods close to even solar cycle maxima, 20 and 22, NS MCs predominate. It can be also observed that for solar minima periods, during the ones preceding odd cycles, SN MCs predominate, while NS MCs predominate for the ones preceding even cycles. The polarity in Y was not analyzed because of the small number of events (15).

Table 2
Distribution of NS and SN MC polarities in function of solar cycle epochs

Solar cycle epoch	NS (%)	SN (%)
Solar minimum 1973–1978	40	60
Solar minimum 1983–1988	80	20
Solar minimum 1993–1998	19	81
Solar maximum 1966–1971	60	40
Solar maximum 1977–1982	38	62
Solar maximum 1987–1992	75	25
Solar maximum 1998–2001	29	71

The MC polarity varies in response to changes in the magnetic structure of their source region. The forward MC fields would be controlled by the polarity of the global solar magnetic field, while the inclination of the coronal streamer belt controls the clouds axial symmetry (Mulligan et al., 1998, 2000). The orientation of the forward MC field is the same as the global dipole solar magnetic field. Fig. 5 shows a sketch of the solar magnetic field and MC polarity for alternate solar cycle. On the left is shown the situation for descending and minimum phases of even solar cycles and ascending and maximum of odd solar cycles; on the right the situation for descending and minimum phases of odd solar cycles and the ascending and maximum of even solar cycles. Close to odd solar cycle maximum the polarity is positive in the solar northern hemisphere while close to the even solar cycle maxima it is positive in solar southern hemisphere. Thus, during odd solar cycle maximum, the predominant polarity of MC should be SN, because the global forward field in the Sun would be to south, while during even solar maximum the polarity predominant of MC should be NS, which is in agreement with the observations. In general, SN MCs occurs more frequently during periods between even and odd solar maxima while NS MCs occur between odd and even solar maxima (Fenrich and Luhmann, 1998).

The results presented in this paper are in agreement with previous works. Zhang and Burlaga (1988) and

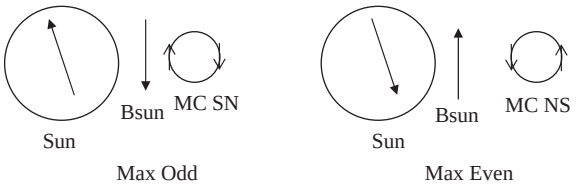

Fig. 5. Relation between the global magnetic field of the Sun and the dominant MC polarity. On the left, solar cycle with positive polarity in the northern hemisphere (odd cycles maximum) and on the right, solar cycle with negative polarity in the southern hemisphere (even cycles maximum).

Bothmer and Schwenn (1998) have studied MCs and found that most of them were SN during 1974–1982 era. Mulligan et al. (1998) studied the 1979–1988 period and they found solar cycle dependence in the B_z signal of bipolar clouds. MC bipolar occurs preferentially during solar minimum to the solar maximum, when the large-scale neutral line and the coronal streamer belt are more flat and equatorial. The peak of unipolar MCs (highly inclined flux ropes) occurs during the declining phase, when the neutral line/streamer belt are highly inclined to the ecliptic. They concluded that MCs are controlled by the large-scale coronal magnetic field of streamer belt. Most cloud structures are not severely inclined with respect to the ecliptic plane (Lepping and Berdichevsky, 2000).

Li and Luhmann (2004) have studied MCs during 1978–2002 period and they have found, during 1978–1982, 9 NS and 22 SN; during 1995–2002, 10 NS and 36 SN; and during 1983–1992, 6 NS and 2 SN. For unipolar MCs, they found, during 1978–1982, 3 N and 4 S; during 1995–2002, 5 N and 13 S. They have found that both, bipolar and unipolar MCs show little trend with solar cycle. During solar cycles 21 and 23, SN MCs predominate. SN MCs during 21 decreases in number with the progress of the declining phase; its polarity seems to reverse, such that SN MC prevails in the last half declining phase and NS MCs continues to increase in occurrence until the following solar maximum. SN clouds increased after the solar minimum 23. However, the small number of events brings difficulties to the interpretation. Li and Luhmann (2004) as well as Mulligan et al. (1998) showed that SN MCs prevails over NS in odd cycles and the reverse is true in even cycles. Thus, the present work results confirm, with a wider database, these previous findings.

The prevailing polarity cases decrease in number towards the solar minimum, while the secondary polarity clouds start to increase in number, only becoming predominant after the later part of the declining phase. Therefore, the predominance of the magnetic cloud polarity reverses within the later part of the declining phase near the solar minimum, but does not coincide with either the solar minimum when the new polarity sunspots begin to emerge or the solar maximum when the large scale solar polar field reverses (Li and Luhmann, 2004).

3.3. Statistics of MC polarity subsets

The average parameters of each MC polarity class are presented in the same format as Table 1, in Tables 3–7, respectively for the data set of MCs SN-Y_+, SN-Y_-, NS-Y_+, NS-Y_- and Y-S. It is seen that, for the same type of Z rotation, there are slight differences between the MC average properties, in function of their Y polarity (as well in relation to the whole set). It is observed that SN MCs present higher average V_{peak} (490–493 km/s) than NS MCs (472–476 km/s) and Y MCs (480 km/s). These differences are lower than the standard deviation, but they could have some physical significance.

The B_{peak}–V_{peak} relation was also obtained for the different polarity MCs data set. Fig. 6 shows the relation between B_{peak} and V_{peak} for NS-Y_+ MCs (top panel on the left), NS-Y_- MCs (top panel on the right), SN-Y_+ MCs (middle panel on the left), SN-Y_- MCs (middle panel on the right) and Y-S MCs (bottom panel). The regression coefficients, a and b, for these 5 MCs classes are presented in Table 8, and the r coefficient for each data set is included in Fig. 6.

A tendency for MCs with higher V_{peak} presenting higher B_{peak} can be also noted for the MC data sets considering polarity. Table 8 presents the values of a and b for the considered subsets. The coefficient a varies

Table 3
Statistics of SN-Y_+ MC parameters

Parameter	Mean/SD	Minimum	Maximum
B_{peak}	16.0 ± 6.3 nT	7.5 nT	35.0 nT
V_{peak}	493 ± 109 km/s	350 km/s	820 km/s
Bs_{peak}	-11.1 ± 6.0 nT	−31.0 nT	−3.3 nT
Dst_{peak}	-92.0 ± 55.4 nT	−240 nT	−33 nT
Perc. (Bs_{peak}/B_{peak})	$69.4 \pm 19.1\%$	24.3%	97.6%

Table 4
Statistics of SN-Y_- MC parameters

Parameter	Mean/SD	Minimum	Maximum
B_{peak}	15.3 ± 6.4 nT	8.0 nT	37.0 nT
V_{peak}	490 ± 114 km/s	345 km/s	788 km/s
Bs_{peak}	-11.0 ± 4.6 nT	−22.7 nT	−4.6 nT
Dst_{peak}	-105.6 ± 54.1 nT	−256 nT	−28 nT
Perc. (Bs_{peak}/B_{peak})	$73.6 \pm 17.8\%$	29.7%	100%

Table 5
Statistics of NS-Y_+ MC parameters

Parameter	Mean/SD	Minimum	Maximum
B_{peak}	13.2 ± 4.5 nT	5.2 nT	23.9 nT
V_{peak}	472 ± 103 km/s	325 km/s	770 km/s
Bs_{peak}	-8.0 ± 3.9 nT	−19.5 nT	−2.4 nT
Dst_{peak}	-84.6 ± 67.5 nT	−288 nT	−5 nT
Perc. (Bs_{peak}/B_{peak})	$60.5 \pm 18.8\%$	15.2%	98.2%

Table 6
Statistics of NS-Y_MC parameters

Parameter	Mean/SD	Minimum	Maximum
B_{peak}	16.5 ± 5.4 nT	8.4 nT	30.9 nT
V_{peak}	476 ± 77 km/s	400 km/s	700 km/s
Bs_{peak}	-11.4 ± 5.3 nT	−212 nT	−3.8 nT
Dst_{peak}	-90.8 ± 42.0 nT	−211 nT	−35 nT
Perc. (Bs_{peak}/B_{peak})	$67.7 \pm 20.0\%$	26.8%	97.5%

Table 7
Statistics of Y-S MC parameters

Parameter	Mean/SD	Minimum	Maximum
B_{peak}	16.6 ± 6.2 nT	7.9 nT	27.0 nT
V_{peak}	480 ± 72 km/s	354 km/s	600 km/s
Bs_{peak}	-10.1 ± 4.4 nT	−16.9 nT	−3.7 nT
Dst_{peak}	-93.8 ± 50.9 nT	−226 nT	−23 nT
Perc. (Bs_{peak}/B_{peak})	$62.1 \pm 19.8\%$	25.0%	96.3%

between 4 and 8 nT for bipolar MCs, but this variation in within the standard deviations. The coefficient b varies between 0.015 and 0.026. For Y MCs the a coefficient is larger and the b coefficient is smaller than the ones obtained previously. Considering the r coefficient, the bipolar MCs present similar correlations, with r in the range 0.37–0.43 (see Fig. 6), which is close to r obtained for the whole data set. These very low correlation coefficients close to 0.4 indicate that less than 16% of the B_{peak} variation could be explained by the linear dependency on V_{peak}. In fact, the results presented here are well below to the ones founded by Gonzalez et al. (1998) and Dal Lago et al. (2001), who obtained correlations of 50% and 36%, respectively. Although the correlation is low and the data points dispersion is large, it is still possible to see that there is a trend to high magnetic field strength events have also high speeds. The high data point dispersion can be explained because the event selection in this work was not so restricted as the one performed in other works, with a larger MC data set including events less well defined than that of Gonzalez et al. (1998).

For Y MCs, the correlation coefficient is even lower, $r = 0.13$. This result could be an indication that the B_{peak}–V_{peak} proportionality is not valid or that it is not maintained for highly inclined magnetic clouds. If the proportionality B_{peak}–V_{peak} is a characteristic only of bipolar magnetic clouds, it could give some hint of a physical mechanism; perhaps the difference being in the ejection of highly inclined and low inclined CMEs. Observational and theoretical/computational studies are needed to check it.

The geoeffectiveness for the MC subset data considering polarity was also investigated. Fig. 7 shows sector graphs with the percentage of magnetic clouds followed by each type of geomagnetic activity conditions for the five subsets: NS-Y_+ (top panel on the left), NS-Y_- (top panel on the right), Y-S (middle panel), SN-Y_+ (bottom panel on the left), SN-Y_- (bottom panel on the right).

As before, the geoeffectiveness is considered by counting the number of intense + moderate storms following each MC class. The occurrence of magnetic activity conditions is slightly different for each class. Nevertheless, the number of geoeffective MCs within each class is comparable with the whole data set (~77%). The class NS-Y_+ presents results slightly different (only 66.6% are geoeffective), since a smaller number of intense storms and a higher number of weak storms followed it, compared to the other subsets. The other MC classes present a distribution similar to the whole set, and between 73% and 85% of these clouds are followed by geoeffective events (73% −SNY_+, 80.0% of Y, 83.3% of NSY_- and 85.7% of SNY_-). Moderate storms are, generally, the most usual type of geomagnetic activity after a MC (around 40%), but intense activity also follows a large percentage of MCs (see Fig. 7). Few MCs are followed by weak activity and an even lower number is followed by quiet conditions. Probably these MCs are the slowest ones, with low speeds and low-magnetic fields. From Fig. 7 it is seen that NS-Y_+ MCs are the less geoeffective, causing less intense storms, although the number of moderate storms is similar to the other MC classes. It is also observed that SN-Y_- and YS clouds are more related to intense storms. However, this result could be masked by the presence, in the case of multiple steps storms, of pre-existing fields in sheath region (Kamide et al., 1998; Vieira et al., 2001).

The type Y_- seems to be more geoeffective for both NS and SN rotation. The importance of the Y-component of the interplanetary magnetic field could be due to the magnetic line reconnection in the magnetopause, although this should be a minor effect. It can be seen that the geoeffectiveness of each MC class is in agreement with the differences observed in MC

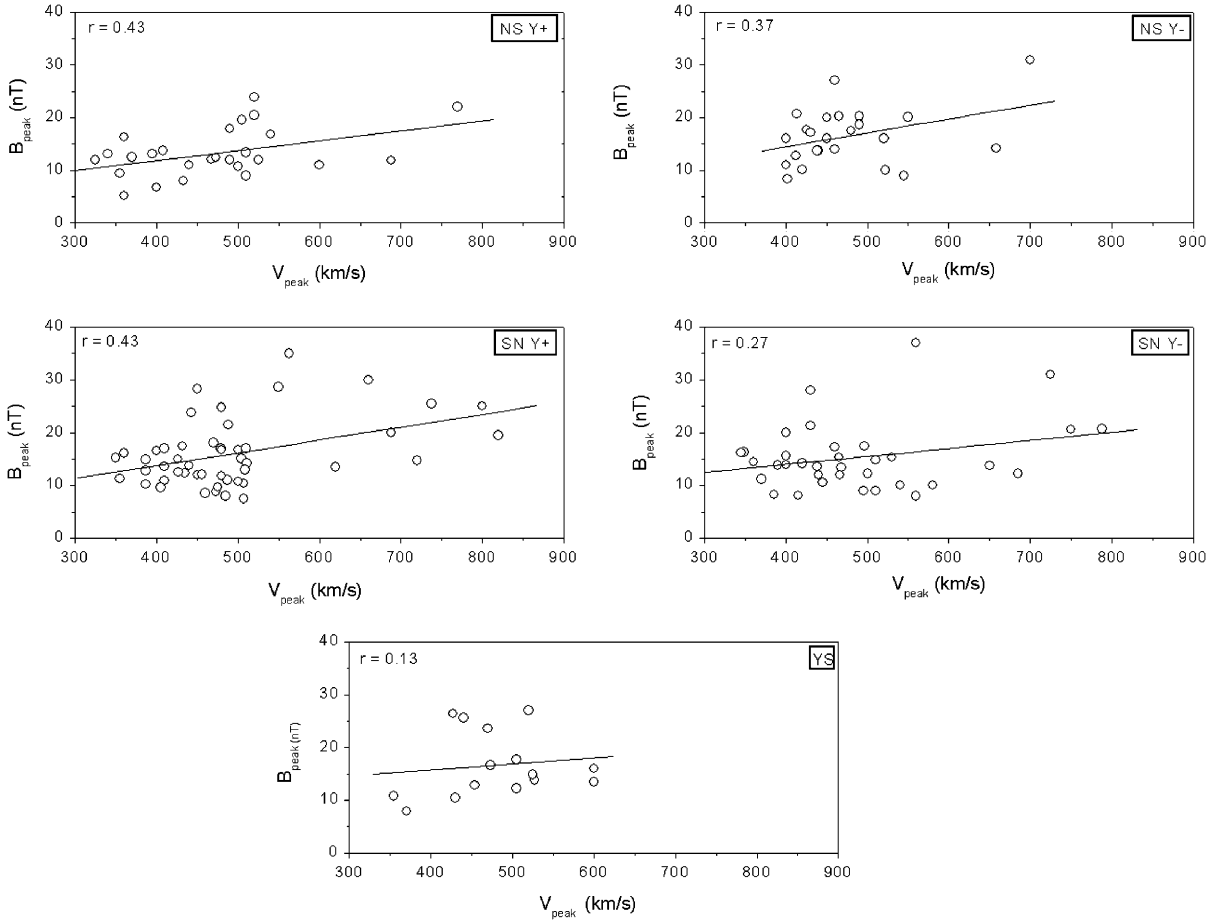

Fig. 6. Relation between B_{peak} and V_{peak} for NS-Y_+ MCs (top panel on the left), NS-Y_- MCs (top panel on the right), SN-Y_+ MCs (middle panel on the left), SN-Y_- MCs (middle panel on the right) and Y-S MCs (bottom panel).

Table 8
Regression coefficients of the B_{peak}–V_{peak} relation for the MCs classes

MC polarity	Coefficient a (nT)	Coefficient b (nT/km/s)
NS-Y_+	4.4 ± 3.8	0.019 ± 0.008
NS-Y_-	3.9 ± 6.7	0.026 ± 0.014
SN-Y_+	3.9 ± 3.9	0.024 ± 0.007
SN-Y_-	7.8 ± 4.7	0.015 ± 0.009
Y	$11.1 + 11.6$	0.011 ± 0.024

parameters (Tables 3–8). The MC SN-Y_- class (Table 4) is the most geoeffective and also the one that shows the highest percentage of southward interplanetary magnetic fields (73%). The MC classes SN-Y_+ and NS-Y_- also show large absolute values of B and B_s. Further, the less geoeffective class, NS-Y_+, presents the lowest average total and southward interplanetary magnetic field. Thus the small statistical differences observed through the average parameters for the different subsets seem to be an indication of true physical differences, which are coherent with each MC class geoeffectiveness.

Klein and Burlaga (1982) have not observed a significant difference in the storm intensity according to the MC class. However, they have observed that the beginning of the storm main phase depends on the MC polarity. Wilson (1987) has also shown that a small fraction of MCs, in spite of having long duration southward magnetic fields, did not cause magnetic storms. Zhang and Burlaga (1988) analyzed 19 MCs observed during 1978–1982 and reported several differences among MCs of different polarities. The number of SN MCs observed by them was higher than of NS MCs, and the SN MCs were associated with periods when solar wind speeds where higher. The disturbances caused by these clouds were of about −100 nT. During the passage of SN clouds, the Dst decrease is due to the forward field regions, while for NS clouds the Dst

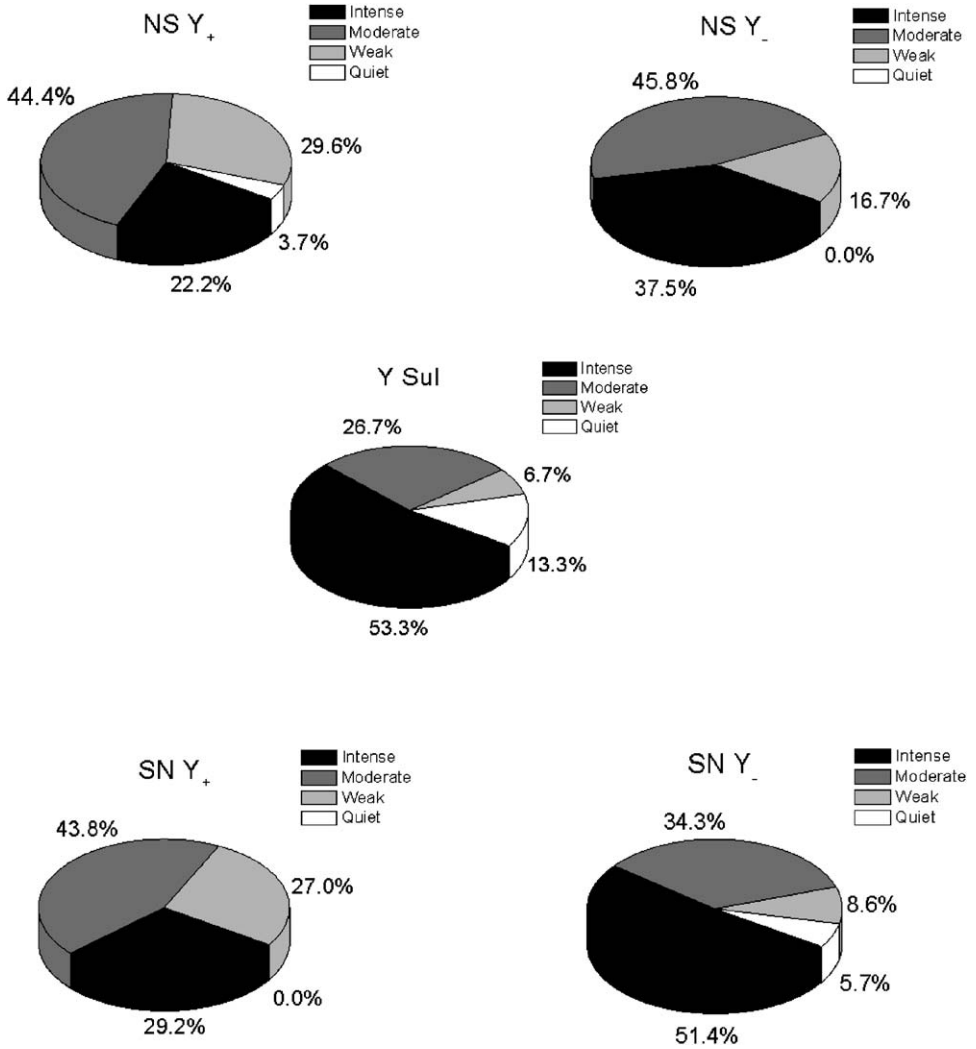

Fig. 7. Graph sector showing the percentage of magnetic clouds followed by each type of geomagnetic activity conditions for the MC class: NS-Y_+ (top panel on the left), NS-Y_- (top panel on the right), Y-S (middle panel), SN-Y_+(bottom panel on the left), SN-Y_- (bottom panel on the right).

decrease occurs due to the rear region fields. Vieira et al. (2002) observed that NS MCs show higher time-integrated values of E_y than SN MCs, i.e., it is necessary more time of energy injection in the magnetosphere for an NS MC causing a given geomagnetic activity disturbance level.

Badruddin (1998), using the same data set of MCs as Klein and Burlaga (1982), separated the MCs in classes led by shocks, followed by CIRs and isolated. He has found that geomagnetic index a_p amplitude was higher for MCs associated with shocks; this is in agreement with which was observed by Echer and Gonzalez (2004) considering MC with shocks and the whole MC data set. Furthermore, Badruddin (1998) has found that a_p is higher for SN clouds in the classes associated with shocks and isolated, and for NS in the class associated with CIRs. The last association might occur because of high-speed compression in MCs, while the former is probably due to sheath effects conjoint with MC fields.

Wu and Lepping (2002a) have studied 34 WIND MCs during 1994–1998 period and they have found that 25% of them were not associated with shocks. They have also determined that from their 34 MCs, ~12% did not have association with storms ($Dst \leqslant -30$ nT), against 3% in the present study. They have also found high correlation between Dst and Bs_{peak}: r~0.77, 0.79 and 0.81 for all, NS and SN clouds, respectively. By considering the total number of storms with $Dst \leqslant -80$ nT during 1964–2000, 261 storms, they found that 22% storms were associated with MCs.

Wu et al. (2003) in an updated study, used 68 MCs observed by WIND during 1994–2002 and they have found that ~91% of MCs were followed by at least weak storms. For the 9% remaining, the spacecraft might have crossed far from the central axis of the MCs.

Li and Luhmann (2004) have studied MCs during 1978–2002 and have selected 25 NS and 60 SN. They observed that Dst_{peak} ranged from −20 to −250 nT for NS and from −20 to −330 nT to SN classes. Thus SN clouds have more intense storms associated with. Also they have observed that 1/3 of moderate or intense storms in that period ($Dst \leqslant -50$ nT) were caused by MCs, while 70% of very intense storms ($Dst \leqslant -200$ nT) were associated with MCs. Li and Luhmann (2004) also found that SN MCs were followed by storms varying from $Dst_{peak} \sim -28$ to −256 nT and NS MCs varying from −5 to −288 nT.

4. Conclusions

A statistical analysis of a 149 MC data set parameters and geoeffectiveness during 1966–2001 period was done in this work. The main results obtained can be summarized as it follows:

- The B_{peak}–V_{peak} relation, first found by Gonzalez et al. (1998), was confirmed for the MC with rotation in Z direction, but it is not conclusive for MCs with rotation in Y direction. The angular coefficient found for the whole data set was however, half of the value found by Gonzalez et al. (1998).
- Overall, 77% of MCs are geoeffective, in the sense that they are followed by intense or moderate magnetic storms, with the percentage of peak southward magnetic field within the clouds reaching 70% of the total magnetic field.
- The geoeffectiveness of MCs varies accordingly to the MC polarity. These differences in geoeffectiveness are in agreement with the differences in the MC parameters. The more geoeffective MC class is the SNY_- type, which has also the highest percentage of the peak southward magnetic field; the less geoeffective class is the NSY_+ class, which has the lowest values of magnetic field strength, southward magnetic field and the peak of B_s. Thus the geoeffectiveness of the MCs is found to be dependent on their intrinsic southward magnetic field intensity, which was expected on the basis of the magnetic reconnection being the main solar wind-magnetosphere energy transfer mechanism.

Acknowledgements

We thank the ACE SWEPAM and MAG teams for making their data available, and the NSSDC at Goddard Space Flight Center for providing the OMNIweb database. The authors would like to thank the reviewers for valuable comments.

References

Badruddin, 1998. Interplanetary shocks, magnetic clouds, stream interfaces and resulting geomagnetic disturbances. Planetary and Space Sciences 46, 1015–1028.

Bame, S.J., Asbridge, J.R., Feldman, W.C., Fenimore, E.E., Gosling, J.T., 1979. Solar wind heavy ions from flare-heated coronal plasma. Solar Physics 62, 179–201.

Blanco-Cano, X., Bravo, S., 2001. Solar wind signatures associated with magnetic clouds. Journal of Geophysical Research 106, 3691–3702.

Bothmer, V., Rust, D.M., 1997. The field configuration of magnetic clouds and the solar cycle. In: Crooker, N., Joselyn, J.A., Feynman, J. (Eds.), Coronal Mass Ejections, Geophysical Monograph 99. American Geophysical Union, Washington, pp. 9–16.

Bothmer, V., Schwenn, R., 1998. The structure and origin of magnetic clouds in the solar wind. Annales Geophysicae 16, 1–24.

Bravo, S., Blanco-Cano, X., 1998. Signatures of interplanetary transients behind shocks and their associated near-surface solar activity. Annales Geophysicae 16, 359–369.

Bravo, S., Aguillar, E., Blanco-Cano, X., Stewart, G.A., 1999. Coronal magnetic structures associated with interplanetary clouds. Solar Physics 188, 163–168.

Burlaga, L.F., 1991. Magnetic clouds. In: Schwenn, R., Marsch, E. (Eds.), The Physics of the Inner Heliosphere. Springer, Berlin, Heidelberg, pp. 1–19.

Burlaga, L.F., 1995. Interplanetary Magnetohidrodynamics. Oxford University Press, New York.

Burlaga, L.F., Sittler, E., Mariani, F., Schwenn, R., 1981. Magnetic loop behind and interplanetary shock: voyager, helios and IMP-8 observations. Journal of Geophysical Research 6, 6673–6684.

Burlaga, L.F., Skoug, R.M., Smith, C.W., Webb, D.F., Zurbuchen, T.H., Reinard, A., 2001. Fast ejecta during the ascending phase of solar cycle 23: ACE observations, 1998–1999. Journal of Geophysical Research 106 (10), 20,957–20,977.

Chapman, S., Ferraro, V.C.A., 1931. A new history of magnetic storms. Terrestrial Magnetism and Atmospheric Electricity 36, 171–186.

Choe, G.S., La Belle Hammer, N., Tsurutani, B.T., Lee, C.L., 1982. Identification of a driver gas boundary layer. EOS Transactions AGU 73, 485.

Crooker, N.V., Gosling, J.T., Kahler, S.W., 1998. Magnetic Clouds at Sector Boundaries. Journal of Geophysical Research 103 (A1), 301–306.

Dal Lago, A., Gonzalez, W.D., Gonzalez, B.T., 2000. Magnetic field and plasma parameters for magnetic clouds in the interplanetary medium. Geofísica Internacional 39, 139–142.

Dal Lago, A., Gonzalez, W.D., Gonzalez, A.L.C., Vieira, L.E.A., 2001. Compression of magnetic clouds in interplanetary space and increase in their geoeffectiveness.

Journal of Atmospheric and Solar-Terrestrial Physics 63, 451–455.

Echer, E., Gonzalez, W.D., 2004. Geoeffectiveness of interplanetary shocks, magnetic clouds, sector boundary crossings and their combined occurrence. Geophysical Research Letters 31, L09808.

Farrugia, C.J., Osherovich, V.A., Burlaga, L.F., 1995. Magnetic flux rope versus the spheromak as models for interplanetary magnetic clouds. Journal of Geophysical Research 100, 12,293–12,306.

Fenrich, F.R., Luhmann, J.G., 1998. Geomagnetic response to magnetic clouds of different polarity. Geophysical Research Letters 25, 2999–3002.

Gold, T., 1959. Plasma and magnetic fields in the solar system. Journal of Geophysical Research 64 (11), 1665–1674.

Gold, T., 1962. Magnetic storms. Space Science Reviews 1, 100–114.

Goldstein, H., 1983. On the field configuration in magnetic clouds. In: JPL Solar Wind Five, pp. 731–733 (SEE N84-13067 03-92).

Gonzalez, W.D., Gonzalez, A.L.C., 1990. Geomagnetic response to magnetic clouds—comment. Planetary and Space Science 36, 1495.

Gonzalez, W.D., Tsurutani, B.T., 1987. Criteria of interplanetary parameters causing intense magnetic storms ($Dst < -100\,nT$). Planetary and Space Science 35, 1101–1109.

Gonzalez, W.D., Lee, L.C., Tsurutani, B.T., 1990. The polarity of magnetic clouds—comment. Journal of Geophysical Research 95, 17,267–17,269.

Gonzalez, W.D., Joselyn, J.A., Kamide, Y., Kroehl, H.W., Rostoker, G., Tsurutani, B.T., Vasyliunas, V.M., 1994. What is a geomagnetic storm? Journal of Geophysical Research 99, 5771–5792.

Gonzalez, W.D., Clúa de Gonzalez, A.L., Dal Lago, A., Tsurutani, B.T., Arballo, J.K., Lakhina, G.K., Buti, B., Ho, C.M., Wu, S.-T., 1998. Magnetic cloud field intensities and solar wind velocities. Geophysical Research Letters 25, 963–966.

Gonzalez, W.D., Tsurutani, B.T., Clúa de Gonzalez, A.L.C., 1999. Interplanetary origin of geomagnetic storms. Space Science Reviews 88, 529–562.

Gonzalez, W.D., Gonzalez, A.L.C., Sobral, J.H.A., Dal Lago, A., Vieira, L.E.A., 2001. Solar and interplanetary causes of very intense geomagnetic storms. Journal of Atmospheric and Solar-Terrestrial Physics 63 (5), 403–412.

Gosling, J.T., 1997. Coronal mass ejections, an overview. In: Crooker, N., Joselyn, J.A., Feynman, J. (Eds.), Coronal Mass Ejections, Geophysical Monograph 99. American Geophysical Union, Washington, pp. 9–16.

Gosling, J.T., Pizzo, V., Bame, S.J., 1973. Anomalously low proton temperatures in the solar wind following interplanetary shock waves: evidence for magnetic bottles? Journal of Geophysical Research 78, 2001.

Gosling, J.T., Baker, D.N., Bame, S.J., Feldman, W.C., Zwickl, R.D., Smith, E.J., 1987. Bidirectional solar wind electron heat flux event. Journal of Geophysical Research 92, 8519.

Gosling, J.T., Bame, S.J., McComas, D.J., Phillips, J.L., 1990. Coronal mass ejections and large geomagnetic storms. Geophysical Research Letters 17, 901–904.

Hirshberg, J., Bame, S.J., Robbins, D.E., 1972. Solar flares and solar wind helium enrichments: July 1965–July 1967. Solar Physics 23, 467.

Kamide, Y., Yokoyama, N., Gonzalez, W.D., Tsurutani, B.T., Brekke, A., Masuda, S., 1998. Two-step development of geomagnetic storms. Journal of Geophysical Research 103 (A4), 6917–6921.

Klein, L.W., Burlaga, L.F., 1982. Interplanetary magnetic clouds at 1 AU. Journal of Geophysical Research 87, 613–624.

Lepping, R.P., Berdichevsky, D., 2000. Interplanetary magnetic clouds: sources, properties, modeling and geomagnetic relationship. Recent Research and Development in Geophysics 3, 77–96.

Lepping, R.P., Berdichevsky, D.B., Wu, C.-C., 2003. Sun–Earth electrodynamics: the solar wind connection. Recent Research and Development in Astrophysics 1, 139–171.

Li, Y., Luhmann, J., 2004. Solar cycle control of the magnetic cloud polarity and the geoeffectieness. Journal of Atmospheric and Solar-Terrestrial Physics 66, 323–331.

Marsden, R.G., Sanderson, R.T.R., Tranquille, C., Wenzel, K.P., Smith, E.J., 1987. ISEE-3 observations of low-energy proton bi-directional events and their relation to isolated interplanetary magnetic structures. Journal of Geophysical Research 92, 11,009–11,019.

Marubashi, S., 1986. Structure of the interplanetary magnetic clouds and their solar origins. Advances in Space Research 6, 335.

Marubashi, S., 1998. Physics of interplanetary magnetic flux ropes: toward a prediction of geomagnetic storms. Proceedings of the International Symposium of CMEs, Tokyo, Japãn.

Mulligan, T., Russelll, C.T., Luhman, J.G., 1998. Solar cycle evolution of the structure of magnetic clouds in the inner heliosphere. Geophysical Research Letters 25, 2959–2962.

Mulligan, T., Russelll, C.T., Luhmann, J.G., 2000. Interplanetary magnetic clouds: statistical patterns and radial variations. Advances in Space Research 26, 801–806.

Neugebauer, M., Goldstein, R., 1997. Particle and field signatures of coronal mass ejections in the solar wind. In: Crooker, N., Joselyn, J.A., Feynman, J. (Eds.), Coronal Mass Ejections, Geophysical Monograph 99. American Geophysical Union, Washington, pp. 245–250.

Owens, M.J., Cargill, P.J., 2002. Correlation of magnetic field intensities and solar wind speed of events observed by ACE. Journal of Geophysical Research 107.

Parks, G.K., 1991. Physics of Space Plasmas, An introduction. Addison-Wesley Publishing Company, Reading, MA, 538pp.

Sugiura, M., 1964. Hourly values of equatorial Dst for the IGY. Annual International Geophysical Year, vol. 35. Pergamon, New York, p. 9.

Tsurutani, B.T., Gonzalez, W.D., Tnag, F., Akasofu, S.-I., Smith, E.J., 1988. Origin of interplanetary southward magnetic fields responsible for major magnetic storms near solar maximum (1978–1979). Journal of Geophysical Research 93, 8519–8531.

Tsurutani, B.T., Goldstein, B.E., Smith, E.J., Gonzalez, W.D., Tang, F., Akasofu, S.I., Anderson, R.R., 1990. The interplanetary and solar causes of geomagnetic activity. Planetary and Space Science 38, 109–126.

Tsurutani, B.T., Gonzalez, W.D., Tang, F., Lee, Y.T., 1992. Great magnetic storms. Geophysical Research Letters 19, 73–76.

Tsurutani, B.T., Gonzalez, W.D., Zhou, X.Y., Lepping, R.P., Bothmer, V., 2004. Journal of Atmospheric and Solar-Terrestrial Physics 66, 147–151.

Vieira, L.E.A., Gonzalez, W.D., Clua de Gonzalez, A.L., Dal Lago, A., 2001. A study of magnetic storms development in two or more steps and its association with the polarity of magnetic clouds. Journal of Atmospheric and Solar-Terrestrial Physics 63, 457–461.

Vieira, L.E.A., Gonzalez, W.D., de Gonzalez, A.L.C., Dal Lago, A., 2002. A study of the geoeffectiviness of southward interplanetary magnetic field structures. Advances in Space Research 30, 2335–2338.

Wilson, R.M., 1987. Geomagnetic response to magnetic clouds. Planetary and Space Science 33, 329–335.

Wu, S.T., Guo, W.P., 1997. Numerical MHD modeling of the solar driver for the destabilization of a coronal helmet streamer. Advances in Space Research 20, 2313–2318.

Wu, C.C., Lepping, R.P., 2002a. Effects of magnetic clouds on the occurrence of geomagnetic storms: the first 4 years of wind. Journal of Geophysical Research 107, 1314.

Wu, C.C., Lepping, R.P., 2002b. Effect of solar wind velocity on magnetic cloud-associated magnetic storm intensity. Journal of Geophysical Research 107, 1346.

Wu, C.C., Lepping, R., Gopalswamy, N., 2003. Variations of magnetic clouds and CMEs in solar activity cycle. In: Wilson, A. (Ed.), Solar Variability as an Input to the Earth's Environemnt, International Solar Cycle Studies (ISCS) Symposium, 23–28 June 2003, Tatranska Lomnica, Slovak Republic, ESA SP-535. ESA Publications Division, Noordwijk, ISBN 92-9092-845-X, 2003, pp. 429–432.

Zhang, G., Burlaga, L.F., 1988. Magnetic clouds, geomagnetic disturbances and cosmic rays decreases. Journal of Geophysical Research 93, 2511.

Zwickl, R.D., Asbridge, J.R., Bame, S.J., Feldman, W.C., Gosling, J.T., Smith, E.J., 1983. Plasma properties of driver gas following interplanetary shocks observed by ISEE-3. Solar Wind Five, NASA Conference Publication CP-2280, p. 711.